

OPTIMIZATION OF 3D PRINTING IN DELTA SYSTEMS: PARAMETERIZATION AND RHEOLOGICAL CHARACTERIZATION FOR FIBER-CEMENT COMPOSITES INCORPORATING OYSTER SHELL POWDER

DOUGLAS SADALLA DE LIRA¹, JUAN CAMILO ADRADA MOLANO¹, RAFAELA ELIAS
RODRIGUES¹, IZABEL CRISTINA FREITAS MORAES¹, HOLMER SAVASTANO JUNIOR¹.

¹*Research Center on Materials for Biosystems – NAP BioSMat, Department of Biosystems Engineering,
University of São Paulo, Pirassununga 13635-900, Brazil.*

ABSTRACT

The 3D printing has revolutionized the manufacture of complex objects in a wide range of sectors, from the construction industry to medicine. The choice of material in 3D printing plays a crucial role in determining the final properties of the object produced. Commonly used inorganic-based materials in this context include clay and Portland cement. Although both are used in additive manufacturing, clay and cement have significant differences in terms of composition, rheological behavior, and applicability in 3D printing. This study investigates the potential of oyster shell powder waste (OSPW) as a rheology modifier to improve the extrusion process of cement-based composites. The objective is to evaluate the feasibility of OSPW in enhancing the extrusion parameters necessary for successful 3D printing of fiber-cement composites using a delta printer. Rheological analysis was conducted through the Benbow-Bridgewater extrusion rheometry technique, measuring key parameters such as flow stress, viscosity and extrusion pressure. Additionally, setting time, open time, fluidity, buildability, and extrudability were assessed to optimize the material for additive manufacturing. The results demonstrate that OSPW improved extrudability and buildability while maintaining the required structural integrity of the printed composites. These findings highlight the potential of OSPW as an ecologically efficient alternative in the development of sustainable fiber-cement composites for 3D printing.

KEYWORDS:

Additive manufacturing; Fiber-cement; Cellulose fiber; Clay; 3D printing cement.

INTRODUCTION

The growing demand for sustainable building materials has driven the search for alternative sources and innovative manufacturing techniques. In this context, fiber cement, widely recognized for its durability and versatility, has been extensively used in various applications in civil construction, especially in building materials with no structural function. However, the conventional production of fiber cement, which relies mostly on cement as a binder, presents significant environmental challenges due to the high carbon emissions associated with the manufacturing process of clinker, the main component of cement (Mehta & Monteiro, 2014). It is estimated that the production of each ton of clinker generates between 800 and 900 kg of CO₂, accounting for approximately 5% to 8% of global anthropogenic CO₂ emissions (Cai et al., 2016; Galusnyak et al., 2022; Lee et al., 2016).

The search for sustainable alternatives has led to interest in using industrial and agricultural waste as components of building materials. One promising example is the use of fillers derived from oyster shell powder waste, an approach that not only reduces environmental impact but also adds value to a commonly discarded waste product (Alvarenga et al., 2012; Expósito et al., 2022). Previous studies indicate that incorporating oyster

shell waste into cementitious matrices can improve the mechanical and durability properties of composites while reducing the carbon footprint of production (Gonçalves & Silva, 2021).

At the same time, rheology plays a key role in 3D printing, an innovative technique that is being explored in the construction industry. The rheological analysis of printing materials, which includes the evaluation of properties such as viscosity, thixotropy, and behavior under different shear conditions, is essential to ensure proper extrusion and accurate deposition of layers during printing (Mostafaei et al., 2021; Zhao et al., 2023). Understanding the rheological parameters of the equipment, such as flow rate and extrusion pressure, is also crucial to optimizing the process, especially considering the maximum pressure limitations of 3 Bar typical of the equipment used (Benbow et al., 1987).

This study proposes the use of oyster shell powder waste as a rheology modifier to facilitate the extrusion of cement-based composites. Through a detailed rheological analysis applying extrusion rheometry techniques, the objective is to explore the potential of this alternative material to enhance the extrusion process, contributing to the development of more ecologically efficient fiber cement composites.

MATERIALS AND METHODS

The fiber cement was manufactured using pozzolanic Portland cement (PPC), due to its optimized composition, which is characterized by a lower clinker content, with sulfate resistance (CP IV 32 - RS) in accordance with Brazilian Standards (NBR 16697 - Portland cement - Requirements, 2018). This type of cement is comparable to Type IP (MS) cement specified in the ASTM Standards (C150 and C595). Oyster shell powder waste (OSPW) was sourced from CYSY Mining (Jaguaruna/SC, Brazil) in commercial form with initial particle sizes between 100 to 1600 μm . The material was processed in a ball mill for 8 h, following the methodology described by Wang and Liu (2020). After milling, the powder was sieved through a Tyler 200 mesh sieve (0.075 mm) to obtain a fine fraction below 75 μm , with approximately 95% of the material passing through the sieve, based on previous research (John et al., 2018; Wang et al., 2018). The particle size distribution of the OSPW (A) and PPC (B) in Figure 1 was achieved using a laser scattering particle analyzer (Malvern MSS Mastersizer) and the median particle sizes (D50) was 19.03 μm and 25.98 μm , respectively.

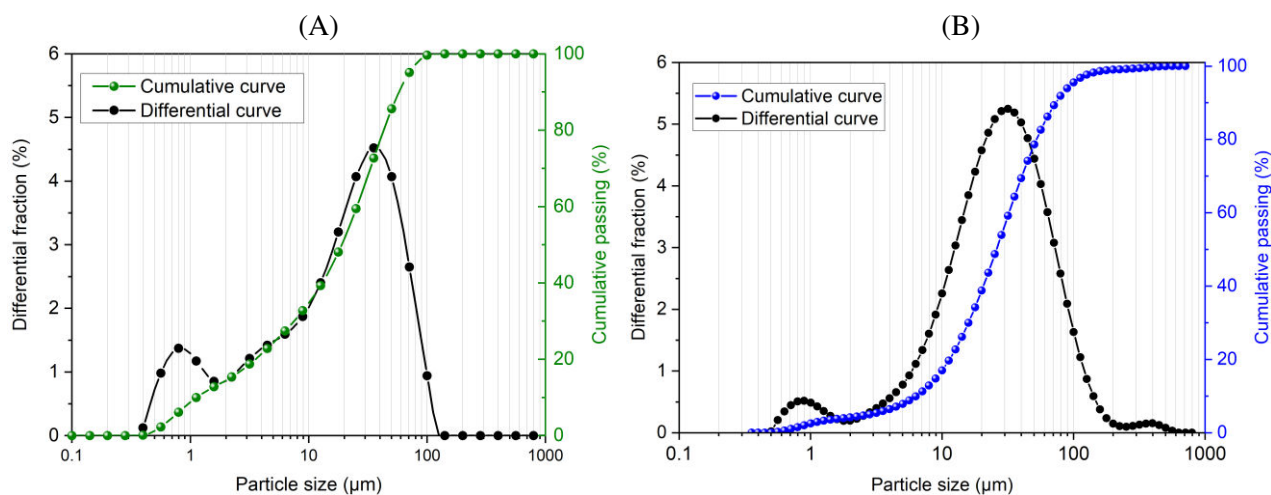


Figure 1 - Particle size distributions of the oyster shell powder waste (A) and pozzolanic Portland cement (B).

Bleached eucalyptus cellulose pulp, supplied by Suzano Paper & Cellulose (Brazil), was incorporated into the fiber cement mixture at a proportion of 3% mass fraction relative to the total dry powder content. The average fiber dimensions of average fiber length (L_c) is 0.791 mm (791 μm) and the average fiber width is 17.66 μm . Three formulations were prepared by varying the proportions of PPC and OSPW, specifically 70% (REF), 40% (PPC40), and 20% (PPC20) of cement, with corresponding OSPW contents of 27%, 57%, and 77% respectively. The water-to-solids ratio was maintained at 0.30 for all mixtures. To optimize the 3D printing process, a polycarboxylate-based superplasticizer (ADVA 527) and a hydroxypropyl methylcellulose-based

viscosity and water retention modifier (HPMC-CELOTEX K15 Premium) were added at a concentration of 1% by mass of the solids.

Granular density was measured with high precision using a helium pycnometer (MVP-6DC Multi Pycnometer, Quantachrome Instruments). The specific surface area of the particles was determined using a surface area analyzer (ASAP 2010, Micromeritics Instrument Corp.) in accordance with the Brunauer-Emmett-Teller (BET) method. The chemical composition of the pozzolanic Portland cement and the oyster shell powder waste was analyzed through X-ray fluorescence (XRF) using a Malvern Panalytical Zetium model. The results are presented in Table 1.

Table 1 – Chemical composition (FRX) of pozzolanic Portland cement (PPC) and oyster shell powder waste (OSPW)

| Samples | Mass Fraction (wt. %) | | | | | | | | | | | | | Density (g/cm ³) | SSA** (m ² /g) |
|---------|-----------------------|------|--------------------------------|------------------|-------------------------------|-----------------|------------------|-------|------------------|------|--------------------------------|------|-------|---------------------------------|------------------------------|
| | Na ₂ O | MgO | Al ₂ O ₃ | SiO ₂ | P ₂ O ₅ | SO ₃ | K ₂ O | CaO | TiO ₂ | MnO | Fe ₂ O ₃ | SrO | LOI* | | |
| PPC | 1.15 | 2.21 | 6.05 | 15.73 | 1.05 | 7.81 | 1.43 | 61.18 | 0.29 | 0.43 | 0.43 | 0.23 | 6.20 | 3.06 | 1.11 |
| OSPW | - | 0.51 | 0.49 | 0.88 | 1.43 | 2.49 | 0.14 | 93.54 | 0.01 | - | 0.01 | 0.41 | 49.00 | 2.82 | 7.34 |

* Loss on ignition at 1020°C.

** Specific surface area (SSA)

A Bruker D8 Advance Eco copper beam diffractometer was used to perform powder X-ray diffraction (XRD) for the mineralogical analysis. A range of Bragg angles (2θ) between 5° and 60° was scanned during the XRD examination under conditions of 25 kV and 40 mA. The scan rate was 0.02° per second. For each scan step, intensity data was collected every second and the diffractometry results were processed using X'Pert HighScore Plus software. The crystallinity and purity of the minerals were confirmed using the Powder Diffraction File database (PDF 2). XRD analysis of PCC revealed the presence of the mineral phases alite (C₃S), belite (C₂S), calcite (CaCO₃), quartz (SiO₂) and muscovite (KAl₂(AlSi₃O₁₀)(OH)₂), in line with the results observed in previous studies, such as those by (Ayub et al., 2021; Singh et al., 2010) and shown in Figure 2. As for the ground oyster waste, the XRD indicated a predominance of aragonite (CaCO₃), a polymorphic form of calcium carbonate. These findings are consistent with the results reported by (Wang & Liu, 2020), who also identified aragonite in oyster shell waste.

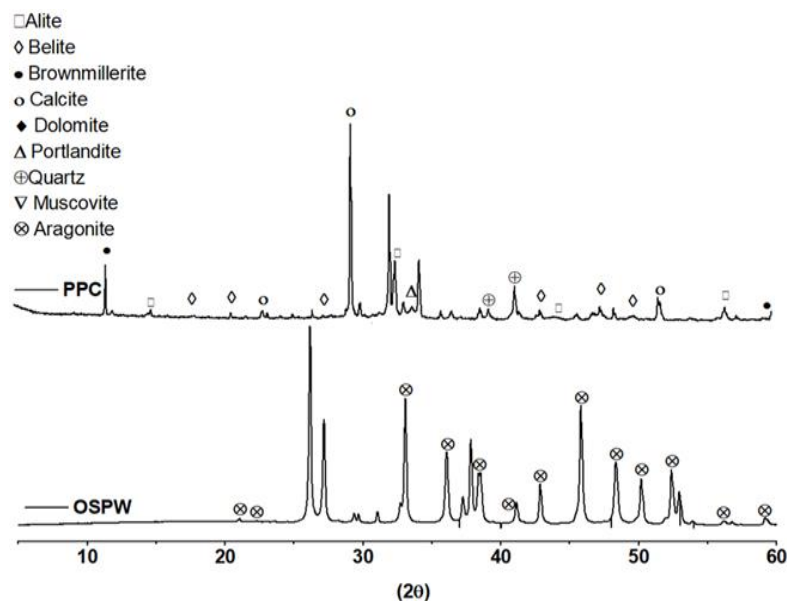


Figure 2 - XRD of raw materials, pozzolanic Portland cement (PPC) and oyster shell powder waste (OSPW).

Morphological analysis was performed using a scanning electron microscope (SEM) Hitachi TM3000 (Tokyo, Japan), while energy-dispersive X-ray spectroscopy (EDS) was conducted using a SwiftED3000 (Oxford Instruments, Abingdon, UK). SEM analysis was carried out at an acceleration voltage of 15 kV. Figure 3

presents the SEM micrographs and corresponding EDS analysis of the raw materials used in the fiber cement composites. Image (a) shows the morphology and elemental composition of the PPC, revealing a heterogeneous distribution of particles; The EDS spectrum indicates the presence of key elements such as Si, Ca, K, Al, Mg, and Mn, typical of cementitious materials. Image (b) displays the SEM image of OSPW, with particles exhibiting irregular morphology and a higher number of fine particles, as shown in the particle size distribution results (Figure 1), compared to PPC. The EDS spectrum highlights the high calcium content, characteristic of calcium carbonate-based materials, along with traces of Na and Al. Finally, image (c) depicts the fibrous structure of the bleached eucalyptus cellulose pulp, with long, interwoven fibers providing a large surface area, which is expected to contribute to the mechanical reinforcement of the composite.

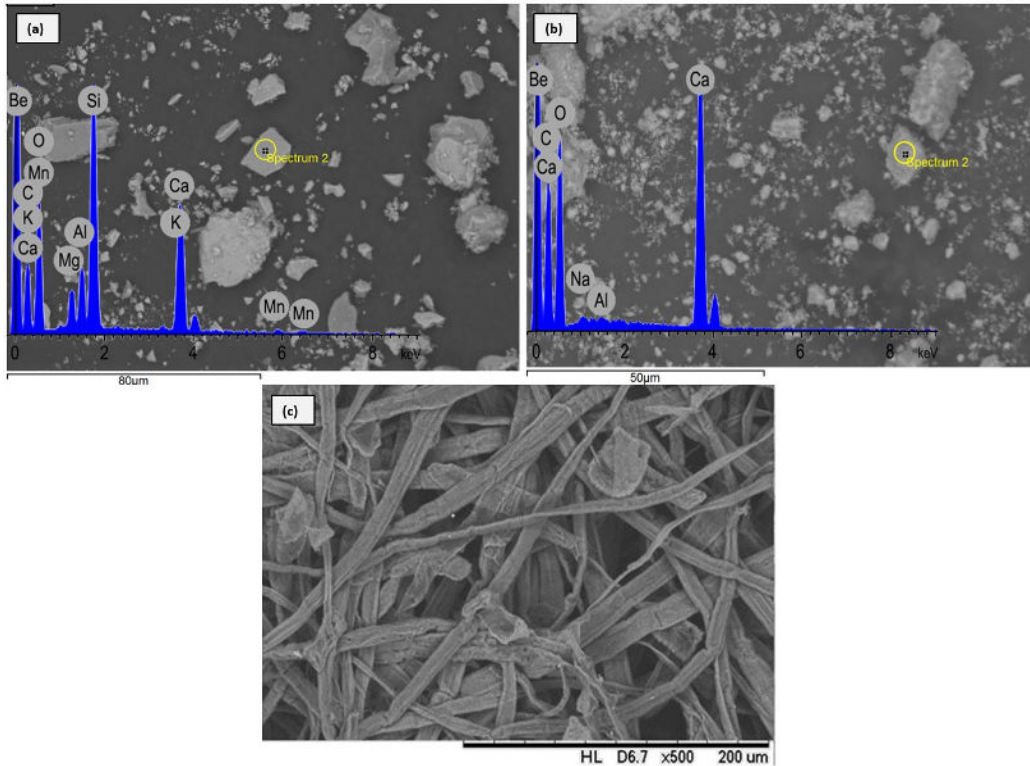


Figure 3 – SEM of the raw materials (a) PPC; (b) OSPW and (c) Eucalyptus bleached pulp.

The rheological test was performed using a universal testing machine (model DL-30.000, EMIC) coupled with an extruder rheometer, following the Benbow-Bridgwater model (1983) for pressure determination, as calculated using Equation (1). The testing procedure adhered to the methodologies described by (Jepthe et al., 2012) (Teixeira et al., 2019), as illustrated in Figure 4. The experiment made use of three nozzles with an internal diameter (D) of 12.7 mm and a barrel with an internal diameter (D0) of 38.10 mm. The lengths (L) of the nozzles were 12.70 mm, 50.80 mm, and 101.60 mm, respectively; this resulted in different L/D ratios of 1, 4, and 8.

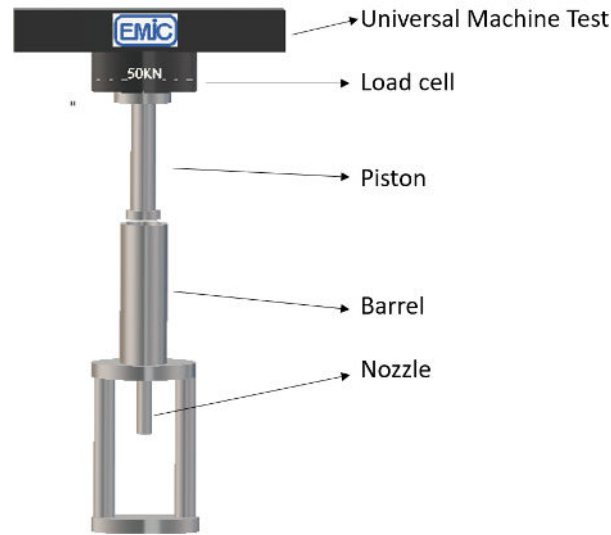


Figure 4 – Lab-scale extruder rheometer coupled to universal testing machine.

The process began with the insertion of a piston into the rheometer cylinder, followed by its connection to a load cell with a capacity of 50 kN. The cylinder was filled completely with fresh fiber cement mixture. The piston was then adjusted so that its lower end was in direct contact with the mixture, establishing the starting point for the test. From this point, the concrete was compressed at constant speeds of 6.5 mm/s, 8.9 mm/s, and 13.3 mm/s, allowing the rheological properties of the material to be characterized under different deformation conditions.

$$P = 2(\sigma_0 + \alpha V) \ln\left(\frac{D_0}{D}\right) + 4(\tau_0 + \beta V) \left(\frac{L}{D}\right) \quad \text{Eq. 1}$$

Where,

P = extrusion pressure;

D_0 = inside diameter of Barrel;

D = inner diameter of the mouthpiece;

L = nozzle length;

V = test speed of the extruder rheometer;

σ_0 = yield stress parameter corresponding to zero speed;

α = is a velocity parameter in the flow stress, which characterizes the effect of velocity at the nozzle inlet;

τ_0 = initial shear stress in the barrel wall, and

β = parameter characterizing the effect of velocity on shear stress.

The mechanical properties of the fiber cement compositions were evaluated 7 days, described by (Filomeno et al., 2023), 2 days of initial cure in saturated conditions and 5 days of thermal curing at 60°C. Seven cubic specimens measuring (50 × 50 × 50) mm³ were tested for compressive strength, in accordance with ASTM C109/C109M-20. For the physical tests, the procedures followed the guidelines outlined in ASTM C948-81(2023), using five specimens of the same dimensions as those used for the mechanical tests.

The 3D printer used for the printing tests was the DuraPrinter E02 (Figure 5). This printer utilizes a delta printing system (refer to Image I). It features mini propeller extruder, and the extrusion nozzle used had a diameter of 2 mm (as shown in Image II). The reservoir operated at a pressure range of 0.2 MPa to 0.65 MPa (Image III).

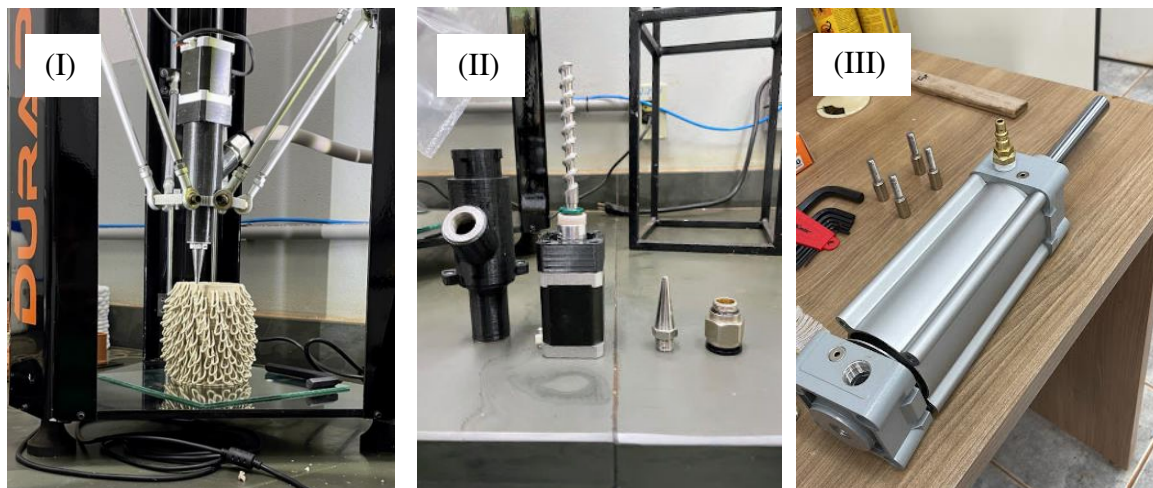


Figure 5 – 3D printer (DuraPrinter E02, model). I. Delta system; II. Mini extruder; III. Reservoir.

RESULTS AND DISCUSSION

The results shown in Table 2 indicate that the compressive strength (MPa) of the fiber cement composites differs considerably comparing the several compositions. The reference (REF) exhibited the highest compressive strength, reaching (42.92 ± 0.83) MPa. On the other hand, the PPC40 and PPC20 mixtures exhibited lower strengths of (26.43 ± 0.76) MPa and (21.67 ± 0.36) MPa. These findings indicate a gradual drop in compressive strength as the replacement of cement with the OSPW increases and also observed according (Kindi et al., 2024; Yigiter et al., 2012).

Table 2 – Compressive strength and physical properties of fiber cement composites.

| Compositions | Compressive strength (MPa) | WA (%) | Porosity (%) | BD (g/cm ³) |
|--------------|----------------------------|------------------|------------------|-------------------------|
| REF | 42.92 ± 0.83 | 12.69 ± 0.19 | 22.71 ± 0.39 | 1.78 ± 0.02 |
| PPC40 | 26.43 ± 0.76 | 15.58 ± 0.10 | 30.04 ± 0.13 | 1.68 ± 0.01 |
| PPC20 | 21.67 ± 0.36 | 19.15 ± 0.23 | 32.19 ± 0.29 | 1.66 ± 0.01 |

Partial replacement of Portland cement with oyster shell waste results in a decrease in compressive strength, attributed to the waste's low reactivity in cement hydration reactions, which causes a decrease in Si, Al and Fe oxides, and an increase especially in Ca oxide. The reduction of available Si may have contributed to the decrease in the formation of C-S-H, which is responsible for the mechanical strength of cementitious materials and has a significant influence on their physical and mechanical properties.

In addition, there is an increase in the porosity and water absorption of the composites. The increase in porosity plays a fundamental role in reducing the mechanical performance and the bulk density and increasing the susceptibility to moisture absorption. These results indicate that oyster shell waste predominantly acts as an inert filler, as expected due to its basic composition of CaCO₃ (Table 1).

The thermogravimetric (TG) curves of the REF, PPC 40 and PPC 20 series, presented in Figure 6, show that the residual mass of the fiber cement incorporated with 57% and 77% oyster powder at 950°C was significantly lower than that observed in the REF sample. This indicates that the addition of oyster powder increased the thermal decomposition of the materials, resulting in a greater loss of mass at high temperatures, due to the greater presence of calcium carbonate (Tu et al., 2016).

The decomposition of portlandite (Ca(OH)₂), typically observed between 400 and 500°C, occurs due to dehydration and the subsequent formation of calcium oxide (CaO). In the pozzolanic Portland cement (PPC) samples, the amount of portlandite is significantly lower compared to the reference sample (REF), suggesting

a possible limitation in the pozzolanic reaction. This phenomenon can be attributed to the addition of oyster powder, which is rich in CaO, particularly in the PPC450 and PCC20 samples. In these samples, the increase in CaO concentration seems to compete with the pozzolanic reaction, resulting in lower portlandite conversion, as also observed in previous studies involving pozzolanic cement composites (Beycioğlu et al., 2016; Korkmaz, 2022).

In the temperature range from 90 to 200 °C, the reduction in mass is mainly due to the evaporation of water physically adsorbed on the surface, together with the initial stages of dehydration of the calcium silicate hydrate structure (C-S-H). Between 250-350 °C is attributed to the thermal degradation of the bleached eucalyptus fibers incorporated into the composite. This temperature range is typical of the decomposition of cellulose and hemicellulose, as noted by (Azevedo & Savastano, 2024).

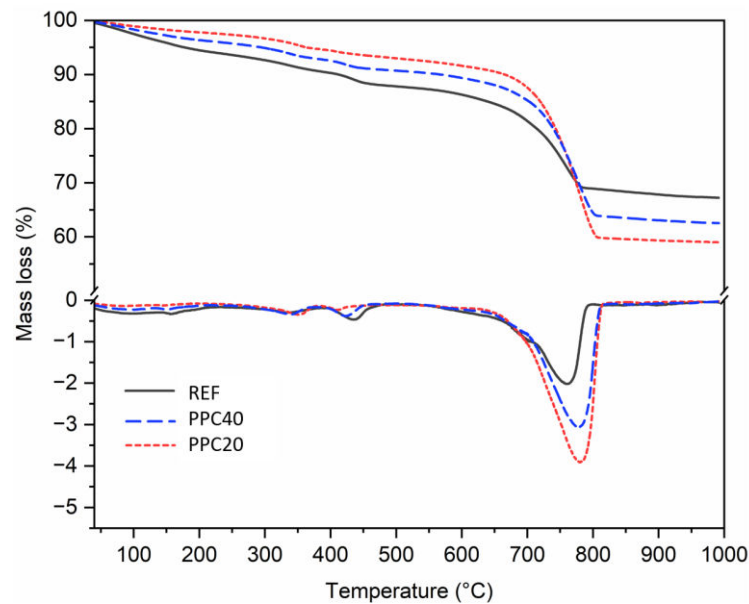


Figure 6 – Thermogravimetric curves (TGA/DTG) of fiber cement composites after 28 days of curing.

The rheological results of the fiber cement mixtures (Table 3), according to the parameters of the Benbow-Bridgewater equation, show that the addition of oyster shell waste (PPC40 and PPC20) significantly reduced the yield stress (σ_0), the yield strength in the matrix (α), the shear stress (τ_0) and the ratio between the shear stress and the strain rate in the material (β), compared to the reference mixture (REF). The bimodal particle size distribution of the OSPW (Figure 1), together with a higher fines content, contributed to a decrease in the viscosity of the PPC40 and PPC20 samples, consequently reducing the total extrusion pressure (P).

Table 3 – Rheological parameter values of σ_0 , α , τ_0 , β and pressures for the fiber cement mixtures.

| Compositions | σ_0 (kPa) | α (kPa/mm.s ⁻¹) | τ_0 (kPa) | β (kPa/mm.s ⁻¹) | p (kPa) |
|--------------|---------------------|---------------------------------------|-------------------|--------------------------------------|------------|
| REF | 222.22 ± 30.51 | 13.07 ± 2.23 | 4.70 ± 3.19 | 0.42 ± 0.20 | 900 ± 42 |
| PPC40 | 68.14 ± 10.22 | 0.56 ± 0.28 | 2.59 ± 0.93 | 0.35 ± 0.06 | 517 ± 21 |
| PPC20 | 30.68 ± 7.95 | 0.29 ± 0.53 | 1.18 ± 0.48 | 0.12 ± 0.04 | 205 ± 10 |

The study conducted an analysis of the rheological parameters using the Benbow-Bridgewater model. The results indicate that the formulations that contain more oyster shell waste (PPC40 and PPC20) significantly reduce the yield stress (σ_0) and initial shear stress (τ_0), (α) and (β) in comparison to the reference mixture (REF). This drop implies that the mixture's internal resistance has decreased and that its fluidity has increased, which will aid in the extrusion process. Changes in extrusion speed have a stronger impact on the reference's

α parameter, which indicates how sensitive the stress is to an increase in strain rate. In contrast, mixtures with more OSPW and fiber content exhibit greater stability.

As OSPW is added, the extrusion pressure (P) decreases noticeably, indicating that the addition of this residue along with the eucalyptus fibers enhances the composite's rheology by assisting in preserving the integrity of the deposited layers, averting collapse, and enhancing structural cohesiveness.

The rheological analysis results were utilized to determine the pressure necessary for printing each fiber cement formulation. Among the formulations tested, only one complied with the safety requirements of the 3D clay printer, which limits the maximum pressure to 300 kPa (~3 bar). The optimal layer heights and extrusion speeds for the printing process were identified through a series of experimental trials. These parameters were adjusted to improve the quality of the printed material, as shown in Table 4.







| Printing speed / Layer height | 1 mm | 1.5 mm | 2 mm |
|-------------------------------|---|--|---|
| 15 mm/s |  |  |  |
| 20 mm/s |  |  |  |

Table 4 – 3D printed cylindrical samples using PPC20 formulation with varying printing speeds and layer heights.

CONCLUSION

The partial replacement of Portland cement with oyster shell waste reduced compressive strength due to its lack of reactivity in hydration while increasing porosity and water absorption. Although mechanical properties were negatively affected, the increased porosity could be beneficial for specific applications such as additive manufacturing, and this material is an alternative to the use of Portland cement, which has high CO₂ emissions. Further studies should explore additive optimization, process scalability, and potential environmental benefits.

Rheological analysis revealed that the fibers were crucial in serving as a structural reinforcer. They improved the mixture's cohesiveness and helped regulate viscosity and fluidity, both of which were essential for maintaining the composite's shape following extrusion. This behavior was necessary to maintain the integrity and dimensional stability of the printed structure by preventing the deposited layers from collapsing during the printing process.

The analysis of Benbow and Bridgwater parameters is essential for the development and optimization of fiber cement mixtures, as it allows the rheology of the material to be adjusted to meet the specific requirements of the printing processes and the equipment. In addition, this analysis makes it possible to predict the behavior of the material during extrusion and deposition. Thus, understanding and applying these parameters contributes to the development of fiber cement composites with rheological properties similar to those of clay.

This study demonstrated the feasibility of applying parameters obtained from clay in a delta 3D printer for the fabrication of fiber cement, with the material's rheology adjusted based on the Benbow model. This approach enabled the successful 3D printing of fiber cement elements, achieving satisfactory mechanical performance. Future research should prioritize the optimization of additive formulations and the scaling of the process for industrial applications.

ACKNOWLEDGMENTS

The authors would like to acknowledge the research funding agencies CAPES, the São Paulo Research Foundation (FAPESP, Processes: 2023/04412-3 and 2014/50948-3), FINEP USPCECO Project (Process #01.22.0267.00, MatMin Call), CNPq INCT (Process 465593/2014-3) and PQ-CNPq (Process 306529/2022-0) for their financial support. Additionally, we extend our thanks to the Graduate Program in Materials Science and Engineering (PPG EnCiMat) at FZEA/USP for providing the instruments and equipment used in this study.

REFERENCES.

- Alvarenga, R. A. F. de, Galindro, B. M., Helpa, C. de F., & Soares, S. R. (2012). The recycling of oyster shells: an environmental analysis using Life Cycle Assessment. *Journal of Environmental Management*, 106, 102–109. <https://doi.org/10.1016/J.JENVMAN.2012.04.017>
- American Society for Testing and Materials (ASTM). (2019). C150/C150M-19: Standard Specification for Portland Cement. West Conshohocken, PA: ASTM International.
- American Society for Testing and Materials (ASTM). (2020). C595/C595M-20: Standard Specification for Blended Hydraulic Cements. West Conshohocken, PA: ASTM International.
- Ayub, M., Othman, M. H. D., Khan, I. U., Hubadillah, S. K., Kurniawan, T. A., Ismail, A. F., Rahman, M. A., & Jaafar, J. (2021). Promoting sustainable cleaner production paradigms in palm oil fuel ash as an eco-friendly cementitious material: A critical analysis. *Journal of Cleaner Production*, 295, 126296. <https://doi.org/10.1016/J.JCLEPRO.2021.126296>
- Azevedo, A. G. S., & Savastano, H. (2024). Assessment of carbonation as a complementary strategy to increase the durability of Magnesium Oxysulfate (MOS)-based fiber cement boards. *Construction and Building Materials*, 438, 137086. <https://doi.org/10.1016/J.CONBUILDMAT.2024.137086>
- Benbow, J. J., Oxley, E. W., & Bridgwater, J. (1987). The extrusion mechanics of pastes—the influence of paste formulation on extrusion parameters. *Chemical Engineering Science*, 42(9), 2151–2162. [https://doi.org/10.1016/0009-2509\(87\)85036-4](https://doi.org/10.1016/0009-2509(87)85036-4)
- Brazilian Association of Technical Standards (ABNT). (2018). NBR 16697: Portland Cement: Requirements. Rio de Janeiro: ABNT.
- Cai, C., Yin, X., He, S., Jiang, W., Si, C., Struik, P. C., Luo, W., Li, G., Xie, Y., Xiong, Y., & Pan, G. (2016). Responses of wheat and rice to factorial combinations of ambient and elevated CO₂ and temperature in FACE experiments. *Global Change Biology*, 22(2), 856–874. <https://doi.org/10.1111/GCB.13065>
- Expósito, N., Rovira, J., Sierra, J., Gimenez, G., Domingo, J. L., & Schuhmacher, M. (2022). Levels of microplastics and their characteristics in molluscs from North-West Mediterranean Sea: Human intake. *Marine Pollution Bulletin*, 181, 113843. <https://doi.org/10.1016/J.MARPOLBUL.2022.113843>
- Filomeno, R. H., Fioroni, C. A., Azevedo, A. G. S., & Savastano, H. (2023). Influence of different curing regimes and accelerated carbonation on the physical, mechanical, and aging performances of fiber cement. *Journal of Building Engineering*, 78, 107791. <https://doi.org/10.1016/J.JOBE.2023.107791>

- Galusnyak, S. C., Petrescu, L., & Cormos, C. C. (2022). Environmental impact assessment of post-combustion CO₂ capture technologies applied to cement production plants. *Journal of Environmental Management*, 320, 115908. <https://doi.org/10.1016/J.JENVMAN.2022.115908>
- Gonçalves, A., & Silva, C. (2021). Looking for sustainability scoring in apparel: A review on environmental footprint, social impacts and transparency. *Energies*, 14(11), 3032. <https://doi.org/10.3390/EN14113032/S1>
- Jepthe, Y., Soto, M., & Paulo, S. (2012). Adaptation of formulations for the production of fiber cement slabs by extrusion. <https://doi.org/10.11606/T.3.2010.TDE-04072012-180623>
- John, V. M., Damineli, B. L., Quattrone, M., & Pileggi, R. G. (2018). Fillers in cementitious materials — Experience, recent advances and future potential. *Cement and Concrete Research*, 114, 65–78. <https://doi.org/10.1016/J.CEMCONRES.2017.09.013>
- Kindi, H. Al, Abdel-Gawwad, H. A., Meddah, M. S., Jabri, K. Al, & Mohamedzein, Y. (2024). An overview of the critical influential parameters on the performance of limestone calcined clay cement paste, mortar, and concrete. *Construction and Building Materials*, 444, 137615. <https://doi.org/10.1016/J.CONBUILDMAT.2024.137615>
- Lee, H.-S., Wang, X.-Y., Tam, V. W. Y., Le, K. N., & Shen, L. (2016). Evaluation of the Carbon Dioxide Uptake of Slag-Blended Concrete Structures, Considering the Effect of Carbonation. *Sustainability* 2016, Vol. 8, Page 312, 8(4), 312. <https://doi.org/10.3390/SU8040312>
- Mehta, P. K., & Monteiro, P. J. M. (2014). *CONCRETE: MICROSTRUCTURE, PROPERTIES AND MATERIALS* (N. Pagan. Hasparyk, Ed.; 2 ed.). IBRACON.
- Mostafaei, A., Elliott, A. M., Barnes, J. E., Li, F., Tan, W., Cramer, C. L., Nandwana, P., & Chmielus, M. (2021). Binder jet 3D printing—Process parameters, materials, properties, modeling, and challenges. *Progress in Materials Science*, 119, 100707. <https://doi.org/10.1016/J.PMATSCI.2020.100707>
- Singh, B., Garg, S. K., Sharma, S. K., & Grewal, C. (2010). Lean implementation and its benefits to production industry. *International Journal of Lean Six Sigma*, 1(2), 157–168. <https://doi.org/10.1108/20401461011049520/FULL/XML>
- Teixeira, R. S., Santos, S. F., Christoforo, A. L., Savastano, H., & Lahr, F. A. R. (2019). Extrudability of cement-based composites reinforced with curauá (*Ananas erectifolius*) or polypropylene fibers. *Construction and Building Materials*, 205, 97–110. <https://doi.org/10.1016/J.CONBUILDMAT.2019.02.010>
- Tu, Z., Guo, M. Z., Poon, C. S., & Shi, C. (2016). Effects of limestone powder on CaCO₃ precipitation in CO₂ cured cement pastes. *Cement and Concrete Composites*, 72, 9–16. <https://doi.org/10.1016/J.CEMCONCOMP.2016.05.019>
- Wang, J., & Liu, E. (2020). Upcycling waste seashells with cement: Rheology and early-age properties of Portland cement paste. <https://doi.org/10.1016/j.resconrec.2020.104680>
- Wang, J., Guo, M., & Tan, Y. (2018). Study on application of cement substituting mineral fillers in asphalt mixture. *International Journal of Transportation Science and Technology*, 7(3), 189–198. <https://doi.org/10.1016/J.IJTST.2018.06.002>
- Yigiter, H., Aydin, S., Yazici, H., & Yardimci, M. Y. (2012). Mechanical performance of low cement reactive powder concrete (LCRPC). *Composites Part B: Engineering*, 43(8), 2907–2914. <https://doi.org/10.1016/J.COMPOSITESB.2012.07.042>
- Zhao, K., Su, Z., Ye, Z., Cao, W., Pang, J., Wang, X., Wang, Z., Xu, X., & Zhu, J. (2023). Review of the types, formation mechanisms, effects, and elimination methods of binder jetting 3D-printing defects. *Journal of Materials Research and Technology*, 27, 5449–5469. <https://doi.org/10.1016/J.JMRT.2023.11.045>